Interim results of the H2020 project FITGEN: design and integration of an e-axle for the third-generation electric vehicles

Michele De Gennaro[1], Patrick Buechel[2], Alfredo Primon[3], Oreste Bertini[3], Paolo Pescetto[4],

James Hoyles Page[1]

[1]*AIT Austrian Institute of Technology GmbH, Giefinggasse 2, Vienna, 1210, Austria,*
michele.degennaro@ait.ac.at

[2]*BRUSA Elektronik AG, Neudorf 14, Sennwald 9466, Switzerland*

[3]*Centro Ricerche FIAT SCpA, Strada Torino 50, 10043 Orbassano, Italy*

[4]*Department of Energy "Galileo Ferraris", Politecnico di Torino, Corso Duca degli Abruzzi 24, 10129, Torino, Italy,*

Summary

The aim of the European H2020 project FITGEN is to develop a functionally integrated e-axle, demonstrated on a full electric urban vehicle platform, fit for implementation in the third-generation electric vehicles. The e-axle features a 6-phase synchronous internal permanent magnet electric motor driven by a Silicon-Carbide inverter, coupled with a high-speed transmission and complemented by a DC/DC-converter for both high voltage operation of the electric motor as well as for superfast charging. Preliminary results shows that the adoption of formed litz wire in the stator allow for a filling factor exceeding 50%, and that the design of the motor is capable of peak performance of 135 kW / 170 Nm, achieving at maximum operational speed of 22,500 rpm and a gravimetric power density of 5.2 kW/kg (i.e. above 50% compared to the 2018 industry standard). This paper presents the interim results of the project with an in-focus look at the end-user requirements, vehicle integration, development of the inverter-motor, optimisation of the cooling system group and integration of the on-board charger.

Keywords: battery electric vehicle, inverter, electric drive, cooling, charger.

1 Introduction

Electrification is the macrotrend that has most influenced research and development activities in transport across the last decade. The European Union has invested significant amounts in low-carbon transport technologies under the H2020 research program, with more than 30 billion EUR of public funding invested in transport research and

infrastructure in the period 2014-20. In parallel, the market for electric and hybrid vehicles has begun to exploit its potential. There were more than 7.5 million electric vehicles circulating worldwide in December 2019, with the largest share in China (45%), and 25% equal shares in Europe and US [1], [2]. Recent figures suggest a xEV market share of 6% by 2020, 24% by 2025 and 48% by 2030 [3] with 24 million vehicles per year expected to be sold by 2030 and a global market turnover of greater than 700 billion EUR per year, including 50 billion EUR due to electrified powertrains.

Concerning the technical development of electric powertrains, the trend focuses on increasing the density of performance of their components while decreasing costs. This usually is achieved through increasing the rotational speed of the electric motor and the switching speed of the power modules and converters. In this framework, the European H2020 project FITGEN (Functionally Integrated E-axle Ready for Mass Market Third Generation Electric Vehicles, [4]) aims to develop, prototype and test a functionally integrated e-axle ready for implementation in third-generation electric vehicles (i.e. 2025 and beyond). FITGEN proposes technical advancements under each element of the electric powertrain, featuring a 6-phase Buried-Permanent-Magnet Synchronous Machine (BPM-SM), driven by a SiC-inverter and coupled with a single speed transmission. It is complemented by a DC/DC-converter for high voltage operation of the motor and fast charging of the battery (120 kW-peak), and an integrated AC/DC on-board charger. The project targets early results show: (1) a 40 % increase[1] of the power density of the BPM-SM, i.e. above 5.0 kW/kg with operation at 22,500 rpm and peak efficiency at 96.5%, (2) a 50 % increase[1] of the power density of the SiC-inverter, 22-25 kW/l and peak efficiency at 99%, (3) the implementation of an affordable and integrated fast charge capability, and (iv) a production cost target at 2,000 EUR/unit (2030 market, cost of BPM-SM, power electronics and transmission). Figure 1 shows a schematic of the architecture of the FITGEN e-axle, including the main components and a simplified electrical scheme.
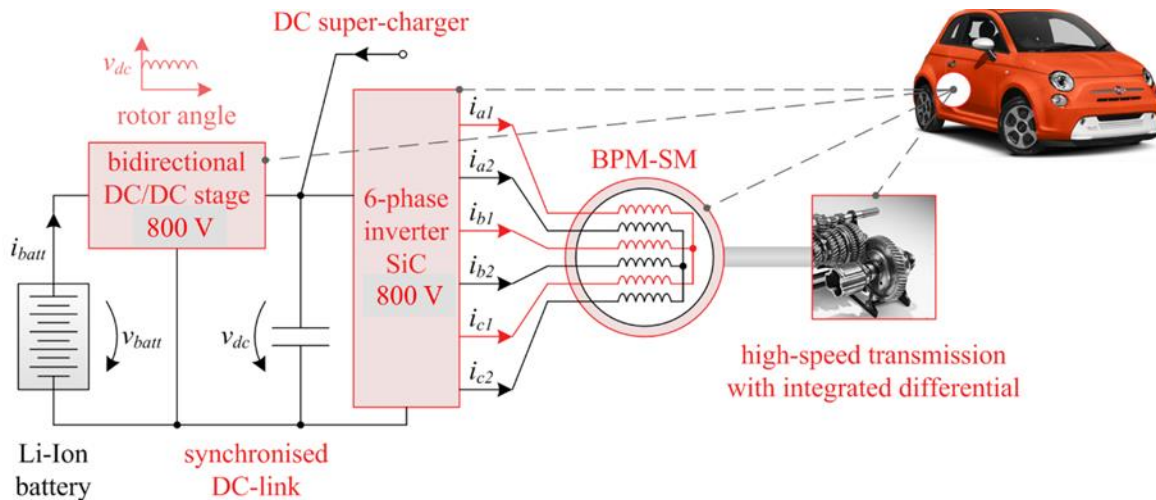

Figure 1: FITGEN e-axle overall architecture
(graphic elements are indicative; the final implementation of the e-axle might change).

FITGEN runs for three years, from January 2019 to December 2021. At the time of submission of this paper, March 2020, the project is in its 15th month, approaching its June 2020 mid-term review. This paper presents its interim results with an in-focus look at the end-user requirements, vehicle integration, development of the e-motor-inverter-transmission group, cooling system design, and integration of the on-board charger.

---

[1] Compared to industry best-in-class technology in the reference year 2018 (i.e. the year when the project was submitted to the EC for funding).

2 End-user requirements and virtual installation of the e-axle in the A-segment vehicle platform

The FITGEN e-axle is intended to be implemented and demonstrated on an A-segment full electric vehicle platform. However, to fully exploit its potential, it has been conceived as multi-platform, considering three reference vehicles for its preliminary sizing: (1) the A-segment full electric vehicle in 2WD configuration planned for its demonstration, (2) a small SUV in plug-in hybrid electric 4WD configuration with the combustion engine on the front axle and the electric traction on the rear axle, and (3) a large SUV full electric vehicle in 4WD configuration with the electric traction on both the front and rear axles. A set of speed profiles, including both type approval (WLTP and US06) and real driving cycles (urban and mixed), have been considered to size the e-axle. Additionally, a highway driving condition at 110 km/h constant speed has been considered, with a target electric driving range of greater than 700 km with one fully charged battery at the beginning plus three stops for fast charging in between. The design condition derived for the e-axle has been identified for the large SUV platform, at a maximum torque of 180 Nm and corner speed of 4,800 rpm. Based on these end-user requirements, the electric motor has been sized and coupled with a single speed transmission unit with a reduction ratio at 1:12.5.

Subsequent to the above identification of the design space of the e-axle components within the demonstrator platform, the e-axle has been virtually installed in the demonstrator. This process accounts for installation of the motor, inverter, transmission, DC/DC converter and associated cabling, considering five different installation options in both front and rear wheel driving configurations. Figure 2 depicts the results of the optimal installation configuration. The group inverter-motor-transmission is integrated as a mono-block (left), on top of which the DC/DC is installed on a supporting frame (centre), minimising the cable length. The e-axle is then mounted in rear wheel driving configuration (right) in the vehicle prototype chassis, using the space in the trunk and applying a mechanical modification to the rear suspension system. This configuration is considered optimal with respect to the requirements of the demonstrator platform (A-segment full electric vehicle), providing the best tradeoff between reduced complexity of the setup, geometric compatibility of the components and frame, and overall performance of the e-axle.
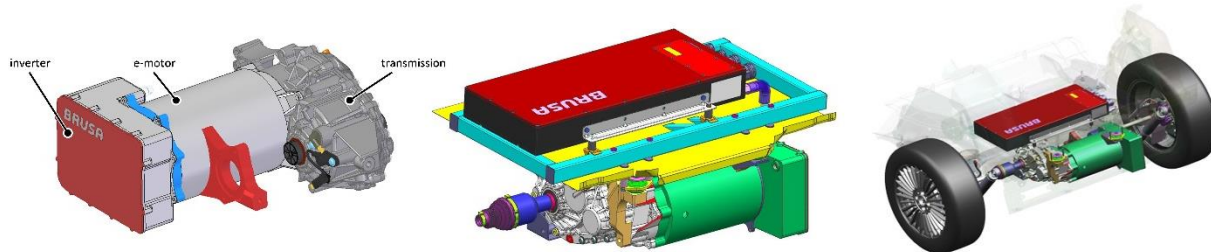

Figure 2: FITGEN inverter-motor-transmission group (left), integration of this group with the DC/DC converter (center) and integration of the full e-axle with the project validator A-segment vehicle prototype rear axle (right).

3 Interim design results of the e-motor – inverter – transmission group

3.1 Inverter

The FITGEN inverter is being designed with the aim of fulfilling various requirements regarding performance, power density and efficiency. A selection of the most important target specifications of the FITGEN inverter is listed in Table 1. The DC-link voltage range is from 520 V to 750 V with a nominal DC-link voltage of 650 V.

Table 1: Target specifications for the drivetrain inverter development.

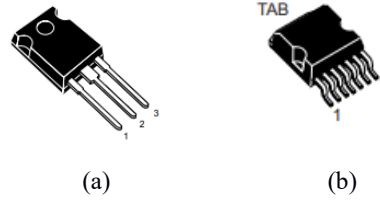| Requirement	Value
Nom. DC-link voltage	650 V
Short time phase current (30 s)	250 A_{RMS}
Cont. phase current	125 A_{RMS}
Switching frequency	8-48 kHz

(a) (b)

Figure 3: The two SiC MOSFETs: a) SCTW100N65G2AG (TO-247 housing) and b) SCTH100N65G2-7AG (TO-263 housing) compared in the study.

A key project goal is the development of the inverter using SiC MOSFETs. This is motivated by the high operation temperature and the low switching losses of the devices. Two SiC MOSFETs provided by ST Microelectronics, SCTW100N65G2AG (TO-247 housing) and SCTH100N65G2-7AG (TO-263 housing), have been analysed regarding their performance in traction inverter application for FITGEN. These are shown in Figure 3. The major difference between the switches is the maximum rated junction temperature which is higher for the TO-247 switch in Figure 3-(a). Therefore, the maximum power dissipated from the Through Hole Technology (THT) device is higher than for the Surface Mount Technology (SMT) device if the same cooling system is used. This allows for a higher drain current per MOSFET. The investigation presented in this paper shows that the housing technology has significant impact on the switching dynamics.

3.1.1 Initial Power Stage Sizing

The initial sizing of the inverter is based on the number of parallel devices per switch to achieve the target performance. This is determined using an in-house MATLAB based design tool. The design tool calculates the average switching and conduction losses of each MOSFET, based on datasheet values as well as the phase current amplitude and the DC-link voltage.

Table 2: Average losses per MOSFET for different numbers of parallel devices per switch with a phase current of 250 A_{rms} and a DC-link voltage per module of 320 V.

	Switching frequency		
Number of devices per switch	$f_{sw} = 12$ kHz	$f_{sw} = 24$ kHz	$f_{sw} = 36$ kHz
3	110 W	117 W	124 W
4	61 W	65 W	70 W
5	39 W	42 W	45 W

The power losses calculated during the initial power stage sizing serve as an input for the system level optimization. The other inputs are the cooling system design, the DC-link capacitor sizing and the machine optimization which are not reported in this paper.

3.1.2 Switching behaviour

The switching behavior of the two devices presented in Figure 3 is also compared via simulation of a double pulse set-up. The test is used to analyze the impact of parasitic inductances in the housings and the bond wires on the achievable switching performance. Figure 4 shows the results of the simulation. The large inductances of the pins of the TO-247 housing result in a slow turn on and turn-off of the device and subsequently large switching loss. The TO-263 device by contrast features significantly lower parasitic inductances and an additional dedicated

driver source pin (Kelvin source). The sum of the turn-on and the turn-off losses are only 38% of the switching losses of the TO-247 device. This shows the importance of an analysis of the parasitic effects for the proper selection of the MOSFET.

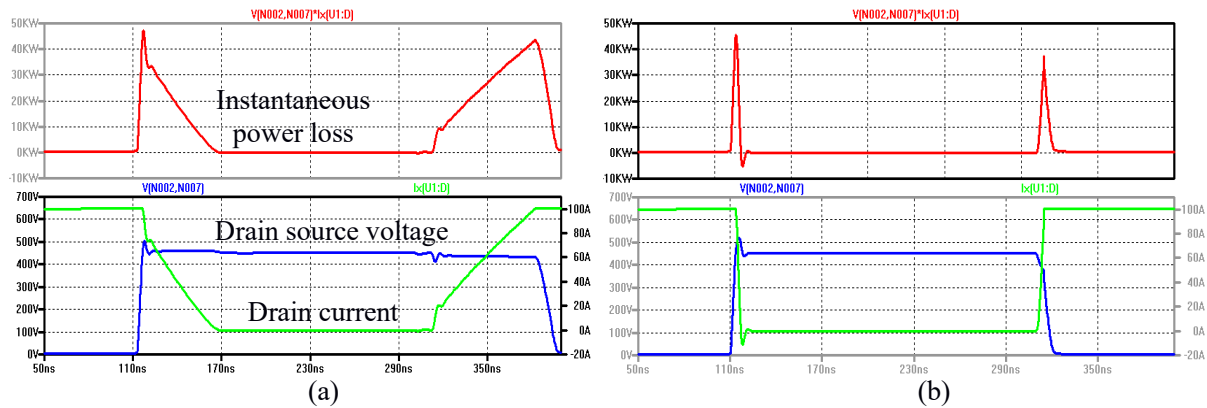(a)   (b)

Figure 4: Simulated switching behaviour of (a) the TO-247 MOSFET and (b) the TO-263 MOSFET showing the switching power loss, the drain source voltage and the drain current.

3.2   Electric Motor

A salient pole buried permanent magnet synchronous motor has been selected for FITGEN (BPM-SM). The machine design is an improvement of the motor developed for the Horizon 2020 project ModulED, [5]. The permanent magnet mass is reduced compared to a surface mount machine reducing the cost of the machine. The machine is designed for a maximum speed of 22,500 rpm and to sustain an overspeed of 27,000 rpm. The high speed allows for 135 kW of maximum power and 170 Nm of maximum torque, achieving a gravimetric power density of approximately 5.2 kW/kg. A novel winding technology using formed litz wire (FLW) is used to allow for a high copper fill factor (exceeding 50%), good thermal properties and a low frequency dependency of the copper losses. This is shown in Figure 5 alongside pull-in winding. The frequency dependency is important due to the high electric frequencies of the high-speed design. The performance of the motor is shown in Figure 6. The peak performance can be sustained for 30s before a derating is required due to the internal temperatures in the machine. The continuous performance can be achieved in thermal equilibrium.
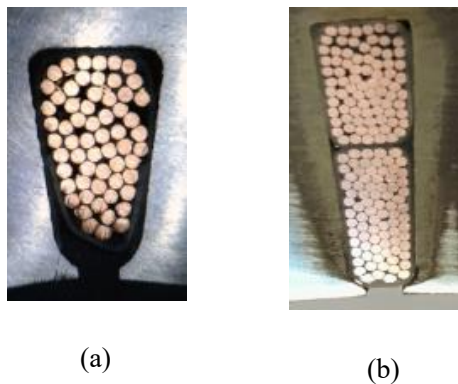

(a)   (b)

Figure 5: Cut through of the winding in the stator slot of a traction drive showing (a) pull-in winding and (b) firmed litz wire winding.
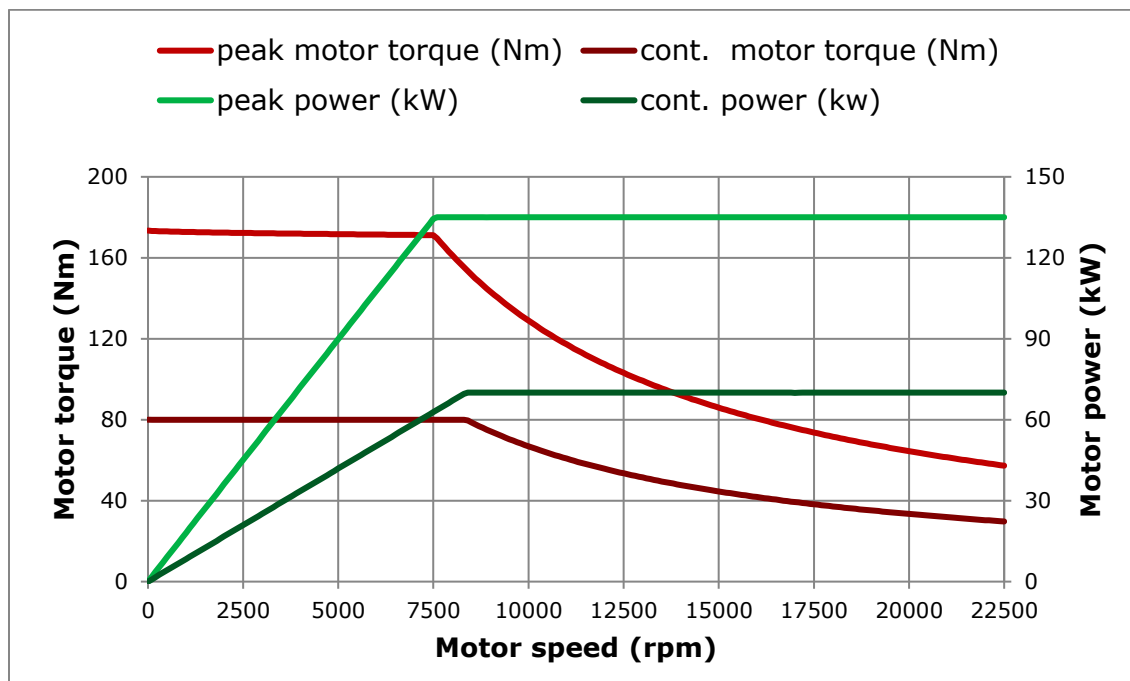
Figure 6: Performance of the FITGEN motor over speed. Peak performance is achieved for 30s and continuous performance is achieved in thermal equilibrium.

4 Liquid cooling system design and optimisation of the group motor-inverter

The liquid cooling circuit will traverse the DC/DC converter, AC/DC inverter and BPM-SM motor in series. The design of each of these three portions is taking place separately, according to a common specified volume flow rate and individually specified pressure drops. This section of the paper gives a brief overview of the CFD-based design and optimization process as applied to the coolant channel in the annulus. The CFD model comprises the rotor geometry, stator geometry, the rotor-stator air gap, idealized cuboidal surrounding air space and coolant channel, as shown in Figure 7 with an interim helical coolant channel design. The cooling channel is specified to exist within an annular spatial boundary inside the external housing which encases the stator. A circular pipe transports liquid coolant to and from the motor annulus.
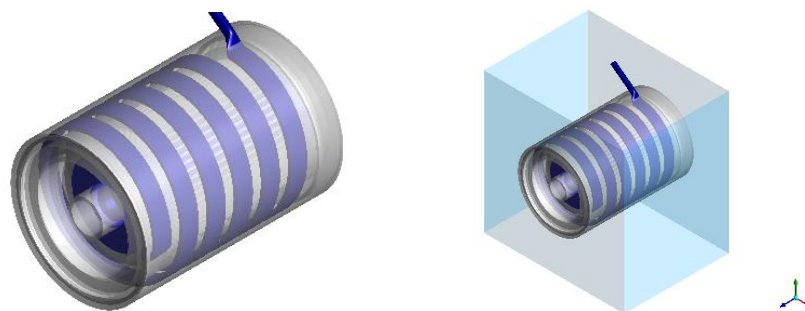

Figure 7: Geometry for the CFD model including rotor and stator (grey transparent), helical coolant channel and air gap (blue), and idealized external air space (light blue) (right hand side).

In order to optimize the coolant channel for the most challenging expected continuous conditions, the prescribed steady drive condition with the maximum rotational speed of 22,500 rpm, combined with the greatest prescribed

outside air temperature is selected for the CFD model setup. Steady total losses in the magnets, rotor iron, winding and stator iron are distributed uniformly throughout the respective parts; design volume flow rate and expected inlet temperature are input at the cooling channel inlet; and a nominal air velocity is applied along the underside of the idealized outside air space. This setup is considered to represent a sufficiently conservative approximation to the worst-case continuous conditions.

The solver used is ANSYS Fluent. The heat flow is solved using the steady energy equation. As the Reynolds numbers for the rotor-stator air gap and external air space are of order 10^4 and for the coolant channel is expected to be in the upper reaches of 2,600 – 10,000, the flow is solved using the steady Reynolds-averaged Navier-Stokes equations with the k-omega SST turbulence model with fully resolved boundary layers. The steady temperature field with a nominal helical coolant channel configuration is shown in Figure 8. The highest temperatures can be found in the mid-axial regions of the rotor and magnets, while the lowest temperatures can be found in the external housing towards the upstream of the coolant channel.
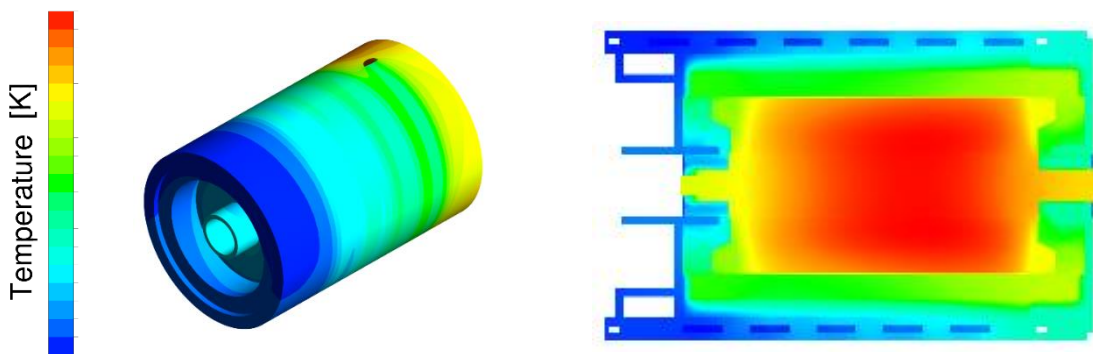

Figure 8: Temperature on the external surface of the motor (left hand side) and on an azimuthal cut (right hand side).

This 3D CFD heat transfer model is currently being used to design and optimize the geometry of the coolant channel to minimize the maximum temperatures in various components, including the magnets and the winding insulation.

Three overall configurations are being considered: helical, axial back and forth, and circumferential back and forth. Each configuration is optimized in turn for comparison. More exotic configurations will not be considered at present. In this paper we will consider the helical configuration which is currently in progress. The helical configuration can be parameterized by the helix angle and channel width. Analogous to the channel width is the wall width between successive helix turns which can be expressed in absolute terms or as a proportion of the maximum non overlapping channel width. As mechanical constraints on the minimum wall width are likely to be applied, the design parameters are selected to be the helix angle and the absolute wall width.

The first part of the design process is a two factor three level full factorial analysis of the design space with factors helix angle and absolute wall width. In the first pass of the design space a wide range of helix angle and wall width has been considered. Figure 9 shows the results for maximum magnet temperature, maximum winding temperature, maximum stator iron temperature and coolant channel pressure drop. There is significant variation in the temperatures with helix angle and almost insignificant variation with wall width. From this, the temperatures can be minimized by maximizing the helix angle within mechanical and pressure drop constraints, which yields the optimal basic design of the helical coolant channel configuration.

The second part of the design process, which is currently underway, is an adjoint-based optimization of the cross-section of the channel with heat transfer and pressure drop as objective variables. Once this is complete, a second design space map similar to that in Figure 9 will be created with the modified cross section, to yield an enhanced design of the configuration. The results will be a well targeted set of options for each configuration, one or more of which will be tested under experimental conditions.
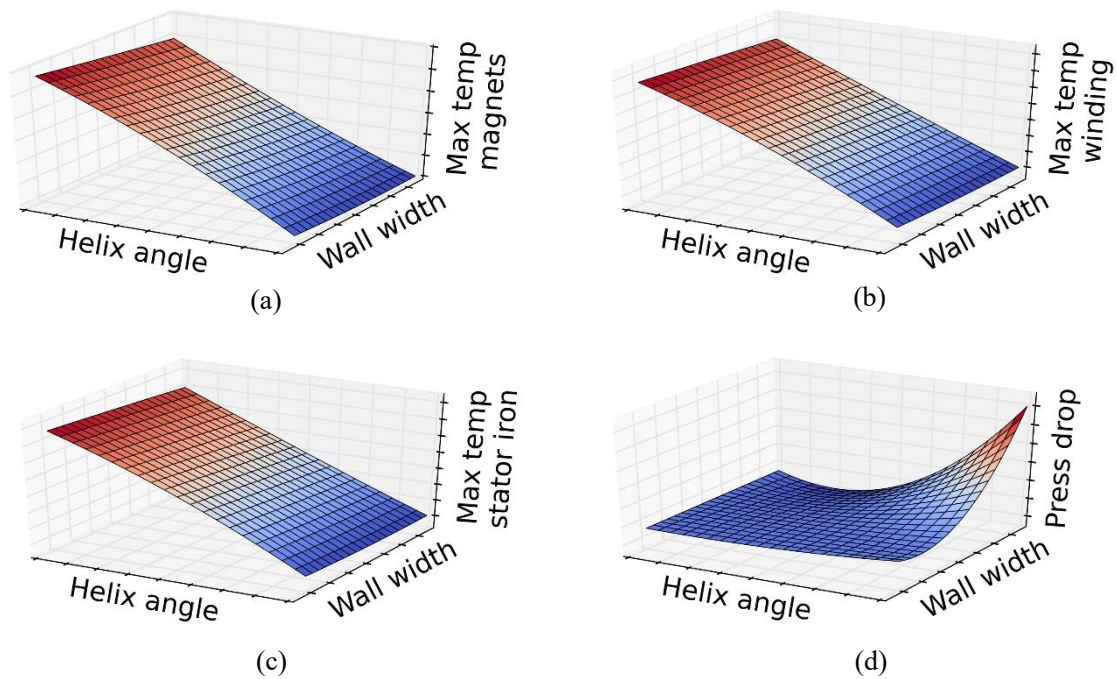
Figure 9: Polynomial surfaces on two factor three level analysis of the helical configuration.

5 Integration study of the on-board charger and fast charging capability

The recent trend of electrification in transportation and the emergence of electric vehicles as a force in the automobile market is being followed closely by the development and deployment of fast and ultra-fast charging stations. The number of these stations is constantly increasing in Europe and USA, both in number as well as in geographical distribution and coverage. Such stations are basically high-power AC/DC rectifiers, with dedicated interface features to enable connection with on-board systems and rapid battery charging of electric vehicles. The increasing charging power capability is necessarily obtained by constantly increasing DC voltage levels, up to 350 kW at 1,000 V as seen with the latest ultra-fast charging stations. Unfortunately, the rapid development of fast-charging stations is not always followed by adequate standardization of voltage levels and connection interface protocols.

A crucial feature of the FITGEN e-axle is the embedded capability to interface with a wide range of high-power DC charging stations, enabling fast battery charging. The target peak charging power set for the project is at 120 kW, with continuous power at 80 kW. Fast charging is enabled by the bidirectional DC/DC converter, which connects the battery (370 V rated) with the 6-phase inverter in driving mode or with a high voltage DC source in charging mode, as can be seen in the drivetrain schematics in Figure 1. The maximum allowed voltage is 750 V, but the DC/DC converter control can adapt to lower levels in order to connect with charging stations of different rated voltage. In absence of specific standards, this makes the FITGEN e-axle compatible with most of the fast-charging converters available at present. An additional feature of the e-axle is the integration of an On-Board Charger (OBC), permitting low- (3-to-6 kW) to mid- (10-to-20 kW) power battery charging from a standard AC grid supply. The conformity to the standards will be a mandatory requirement [6]. A typical charging cycle is split into two parts, nominally Constant Current (CC) and Constant Voltage (CV) control mode. The CC mode is adopted at medium and low battery States Of Charge (SOC), when the battery internal voltage is lower than approximately 90% of its maximum value. In this condition, the maximum (and constant) DC charging current allowed by the OBC is forced into the battery. The battery voltage slowly increases, resulting in slowly decreasing charging power. When the internal battery voltage is close to the maximum value, the OBC works in CV mode,

imposing maximum voltage at the battery input. In this situation, the charging current and power are strongly reduced.

The literature proposes two main solutions for OBCs, nominally stand-alone and integrated topologies. Both these options are being investigated and analysed in the FITGEN project. The first one has the advantage of exploiting well established technologies, while the second one pursues the deepest possible integration with the e-axle. In both cases, it is required that the OBC must be compatible with single- or three-phase grid supply and controlled either in CC or CV mode. For the stand-alone solution, a two conversion stages topology has been selected, with an Active Front-End (AFE) rectifier in series with an isolating DC/DC converter. The basic scheme is reported in Figure 10.
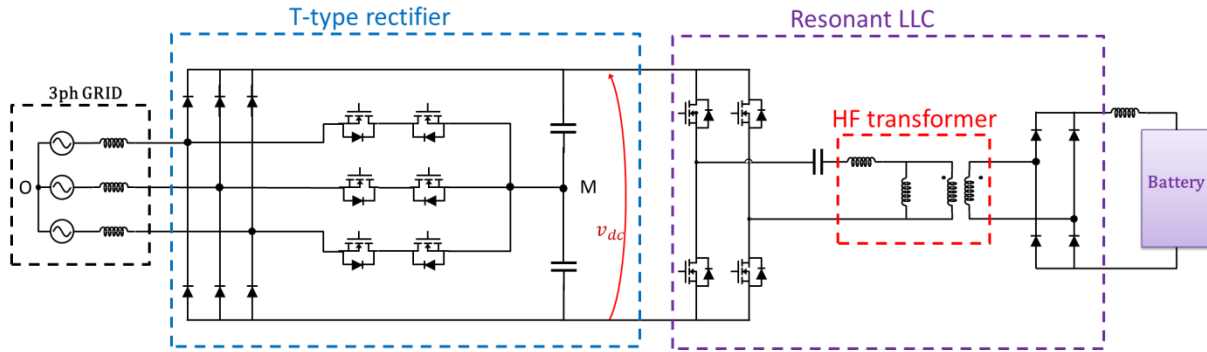

Figure 10: Selected topology for stand-alone OBC.

For the AFE, a 3-level T-type rectifier has been adopted. This topology guarantees a good trade-off between the number of active power electronic components and grid current quality. The rectified voltage v_{dc} has been adopted to feed a resonant LLC converter, composed of an H-bridge, a capacitor and an HF transformer. The H-bridge switches are controlled with fixed duty cycle (d=0.5), but variable switching frequency f_{sw}. Such switching frequency is close to the resonance frequency of the series between the capacitor and the magnetizing inductance of the HF transformer ($\approx$ 20 kHz). Therefore, the regulation of f_{sw} permits regulation of the output voltage of the transformer, which is rectified by a simple diode bridge, and regulation of the battery side voltage and current amplitude. This permits operation of both in CC and CV mode. On the other side, the integrated solution aims to improve the compactness of the system and reduce weight and volume of the OBC. Considering the e-axle topology of Figure 1, the basic idea is to use the motor itself as passive reactive element (inductor) and the traction inverter as a power electronic conversion unit. Several integrated OBC topologies were proposed in previous literature for standard 3-phase machines [7], which have not seen significant adoption by car makers [8]. Multiphase machines, such as the 6-phase motor developed for the FITGEN project, open a wide array of possibilities in terms of topologies and control strategies [9].

6 Conclusions

This paper presents an interim snapshot of the activities and results of the H2020 project FITGEN, as per project month 15 (March 2020) out of 36. Focus is made on the public results available in the areas of definition of the end-user requirements, vehicle integration, development of the inverter-motor, optimisation of the cooling system group and integration of the on-board charger. Preliminary results show that the FITGEN e-axle is likely to outperform the best-in-class electric traction technology in the 2018 in several areas, delivery a state-of-the-art functionally integrated traction system demonstrated on a A-segment passenger car. Future works will focus on the further advancements in the inverter area, cooling system, drive control and demonstration on the vehicle.

Acknowledgments

References

[1]   https://www.iea.org/reports/tracking-transport-2019/electric-vehicles (Retrieved March 2020).

[2]   http://www.ev-volumes.com/ (Retrieved March 2020).

[3]   Boston Consulting, *The future of Battery Production for Electric Vehicles,* 2018.

[4]   www.fitgen-project.eu (Retrieved March 2020).

[5]   https://www.moduled-project.eu/ (Retrieved March 2020).

[6]   International standard IEC 61851.

[7]   M. Yilmaz and P. T. Krein, "Review of Battery Charger Topologies, Charging Power Levels, and Infrastructure for Plug-In Electric and Hybrid Vehicles," in *IEEE Transactions on Power Electronics*, vol. 28, no. 5, pp. 2151-2169, May 2013.

[8]   Su, Gui Jia. "Electric vehicle system for charging and supplying electrical power". US Patent No. US7733039B2, filed September 21, 2007, issued June 8, 2010.

[9]   I. Subotic, N. Bodo, E. Levi, B. Dumnic, D. Milicevic and V. Katic, "Overview of fast on-board integrated battery chargers for electric vehicles based on multiphase machines and power electronics," in IET Electric Power Applications, vol. 10, no. 3, pp. 217-229, 3 2016.

Presenter Biography

Michele DE GENNARO has a Ph.D. in Aerospace Engineering and a postgraduate Master in Research and Innovation Management. He is a Senior Scientist at AIT, and, previously, he was Scientific Officer at the European Commission's DG Joint Research Centre and expert for DG Research and Innovation. He is author of 50+ scientific articles, of which more than 15 are in highly ranked scientific journals. He is currently coordinator of the 5.8 million EUR EU H2020 project FITGEN (https://cordis.europa.eu/project/rcn/218519/factsheet/en). His research interests embrace a wide range of topics, including electric and hybrid vehicles, energy storage technologies, big data studies on mobility, drivetrain design, battery durability, green aircraft propulsion systems and various electric aircraft technologies.